International Journal of Mass Spectrometry 304 (2011) 36–40

Contents lists available at ScienceDirect

International Journal of Mass Spectrometry

journal homepage: www.elsevier.com/locate/ijms

Simulation of duty cycle-based trapping and ejection of massive ions using linear digital quadrupoles: The enabling technology for high resolution time-of-flight mass spectrometry in the ultra high mass range

Jeonghoon Lee[a], Maxwell A. Marino[b], Hideya Koizumi[c], Peter T.A. Reilly[a,*]

[a] Department of Chemistry, Washington State University, Pullman, WA 99164-4630, United States
[b] Colorado College, Colorado Springs, CO 80903, United States
[c] Arkansas State University, State University, AR 72467, United States

ARTICLE INFO

Article history:
Received 16 February 2011
Received in revised form 25 March 2011
Accepted 26 March 2011
Available online 4 April 2011

Keywords:
Ultra high mass
High resolution
Time-of-flight
Duty cycle
Digital ion guide

ABSTRACT

Duty cycle-based trapping and extraction processes have been investigated for linear digitally driven multipoles by simulating ion trajectories. The duty cycles of the applied waveforms were adjusted so that an effective trapping or ejection electric field was created between the rods and the grounded end cap electrodes. By manipulating the duty cycles of the waveforms, the potentials of the multipole rods can be set equal for part of the waveform cycle. When all rods are negative for this period, the device traps positive ions and when all are positive, it ejects them in focused trajectories. Four Linac II electrodes [1] have been added between the quadrupole rods along the asymptotes to create an electric field along the symmetry axis for collecting the ions near the exit end cap electrode and prompt ejection. This method permits the ions to be collected and then ejected in a concentrated and collimated plug into the acceleration region of a time-of-flight mass spectrometer (TOFMS). Our method has been shown to be independent of mass. Because the resolution of orthogonal acceleration TOFMS depends primarily on the dispersion of the ions injected into the acceleration region and not on the ion mass, this technology will enable high resolution in the ultrahigh mass range (m/z > 20,000).

1. Introduction

Since the development of the use of electrospray [2] and matrix-assisted laser desorption [3] to mass analyze large biomolecules, scientists have been trying to improve the range of mass spectrometers. Currently available mass spectrometers work well for analysis of analytes with molecular weights up to roughly 20,000 Da [4]. While it is true that mass measurements in the 100–1000 kDa range abound in the literature [5–8], it is clear that resolution, mass accuracy and sensitivity rapidly deteriorate with increasing mass beyond 20 kDa. Consequently, the exact cut off or limiting range of mass spectrometers is arguable because it really depends on analytical needs. However, the mass-related loss of resolution, sensitivity and mass accuracy is a tangible issue.

The fundamental reason for the deterioration of the analysis with increasing mass is the expansion-induced kinetic energy. Both the average and the spread of the distribution increase monotonically with mass [9]. These attributes are detrimental to the mass analysis beyond 20 kDa. The net effect of the increase in the kinetic energy with mass is a reduction in the ability to capture the analytes in trapping instruments or a reduction in the resolution, mass accuracy and sensitivity in instruments where the ion trajectories define the mass.

It is possible to shift the average energy of the distribution with a well placed electric field; however, the spread of the distribution will remain an issue and the dispersion of the ions will generally continue. The net result is that a small fraction of the ions can have their trajectories adjusted to acceptable values, but there will be a continuum of ions present whose trajectories have not been appropriately adjusted and can interfere with the mass measurement of the small adjusted fraction.

In 2004, Chernushevich and Thomson [8] used collisional cooling after the expansion into the main chamber to "stop" the massive ions (~650 kDa). They increased the pressure in the first quadrupole ion guide up to 40 mTorr to damp the forward motion and radial oscillations before the ions were transmitted to the next multipole device. This process removed the expansion-induced kinetic energy and markedly improved the TOF signal intensity of the massive multiply charged ions. Unfortunately, the resolution achieved in the vicinity m/z = 28,000 was roughly 200 ($m/\Delta m$). Chernushevich and Thomson [8] used an orthogonal acceleration time-of-flight mass analyzer (oa-TOFMS). This analyzer operates on the premise that

* Corresponding author. Tel.: +1 509 335 0042.
E-mail address: pete.reilly@wsu.edu (P.T.A. Reilly).

1387-3806/$ – see front matter © 2011 Elsevier B.V. All rights reserved.
doi:10.1016/j.ijms.2011.03.011

Fig. 1. Equipotential contour plots of (a) a quadrupole ion guide with +500 V and −500 V on each rod pair with equipotential lines at ±400, 300, 200, 100, 50, 20 and 5 V. (Right) An enlarged view of the fringe contours at the exit. (b) Contour plot with all for rods at +500 V with equipotential lines at +400, 300, 200, 100, 50 and 20 V. (Right) An enlarged view of the focusing potential contours at the exit.

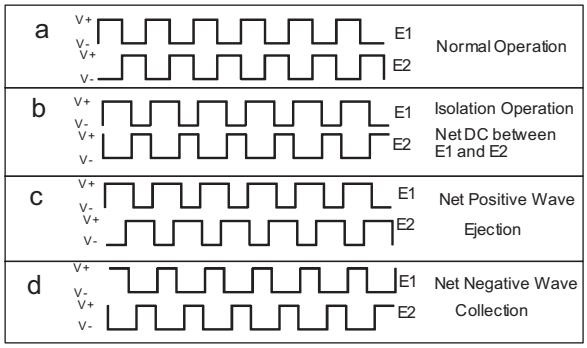

Fig. 2. (a) 50/50 duty cycle waveform typically used for a digital ion guide. (b) 60/60 duty cycle used to create a DC potential between the rod pairs for ion isolation. (c) 60/40 duty cycle used to create a positive potential between all four rods and the end cap electrodes for 20% of the waveform cycle used to axially eject the ions in a collimated beam. (d) 40/60 duty cycle used to create a negative potential between all four rods and the end cap electrodes for 20% of the waveform cycle used to trap ions.

the ions are injected into the accelerator region with the correct kinetic energy/charge ratio (KE/z) and trajectories that are orthogonal to the acceleration vector [10,11]. Under those conditions, high resolution is achievable. Most importantly, high resolution should be achievable at any mass-to-charge ratio (m/z) provided the dispersion of the ion trajectories into the acceleration region does not change.

Stopping the ions in the first quadrupole permits instrumental control of the KE/z during the ion injection process; however, it does not guarantee orthogonal ion trajectories into the accelerator region. It is the dispersion of the ion injection that limits and defines the resolution of the oa-TOFMS in the experiments of Chernushevich and Thomson [8]. Guilhaus [12] explains this as an issue of the turnaround time. Two ions starting out at the same distance from the detector in the acceleration region but moving with same speed but in opposite directions along the TOF axis will reach the same velocity in the drift region. The turnaround time provides the greatest contribution to Δt at the detector when the ion injection is dispersive and roughly defines the flight time difference (Δt) at the detector. The great difference between the resolution achieved in the low mass range relative to the ultra high mass range ($m/z > 20{,}000$) suggests a mass dependence of the dispersion of the ions as they exit multipole ion guides. A better way of trapping and axially ejecting ions from multipole devices is needed to obtain high resolution and sensitivity in the ultra high mass range ($m/z > 20{,}000$).

This work simulates the use of digitally derived waveforms to trap and collect ions in linear multipoles and then promptly eject them on-demand from the device in well-collimated trajectories into the acceleration region of an oa-TOFMS. Our methodology works well at any mass. It is therefore the enabling technology for yielding high resolution TOF mass spectra in the ultra high mass range.

2. Theory

The potential contours of a typically operating linear quadrupole ion guide are depicted in Fig. 1(a) where each opposing rod pair has a positive and negative potential while the end cap electrodes are grounded. An enlargement of the fringe field region is show on the right of Fig. 1(a). Toward the center of the device the potential contours appear as lines that run parallel to the quadrupole electrodes. The central line represents the zero potential line. If the ions travel along the central axis without deviation, then they will pass through and out of the device in a straight line unaffected by the electric fields. As the ions moves away from the central line, they experience an increasing restoring force normal to the potential contours toward the central axis. It is that force that keeps them collimated. The fringe fields arise between the quadrupole rods and the end cap electrodes of the device. They are represented in Fig. 1(a) by the curved equipotential lines at the ends of the rods. When the ions stray off the central axis in the fringe region they encounter a force that pushes them out and back toward the central axis without encountering the same restoring force thereby creating their dispersive trajectories. It is the fringe fields that create the dispersive trajectories out of the quadrupole.

Fig. 1(b) presents the unusual situation where all 4 quadrupole electrodes are at the same potential with the end cap electrodes at ground. Under these conditions, there are no potential contour lines within the center of the device. There is no electric field there because the ions "see" the same potential all around them and they are free to diffuse out of the device. At the ends of the device where the rods are interacting with the end cap electrodes equipotential lines abound. The depicted contours are reminiscent of an Einsel lens, a device used for focusing charged particles. An enlargement of the focusing potential contours is shown to the right of Fig. 1(b). Ions that pass through those fields will be focused toward the central axis.

The potentials depicted in Fig. 1(a) and (b) yield opposite effects on the ions. The first yields collimation (focusing) of the charged particles in the middle and dispersion (defocusing) as they exit the device. The second yields dispersion when the charged particles are in the middle and focusing at the exits. If the positive attributes of both these depictions could be combined, we would have what is needed for injecting the ions in a well-collimated line into the acceleration region of the oa-TOFMS. This can be done by digitally time-sharing the potentials. For most of the time the device is operating as a "normal" digitally driven quadrupole ion guide with the potentials on the opposite rods switching between + and $-V$ and for a smaller fraction of the time all four rods operate at the same potential.

This process is schematically shown in Fig. 2. Under normal digital operation as an ion guide (Fig. 2(a)), the rod potential waveforms E1 and E2 have a 50% duty cycle and are opposite in phase. For 50% of the cycle rod set E1 is high (+V) while set E2 is low (−V) then both sets switch at the same time yielding E1 low (−V) and E2 high (+V) for the rest of the cycle. However the duty cycle of the waveforms can be digitally changed. In Fig. 2(b), we depict the use of digital asymmetric waveforms to perform ion isolation. By setting the duty cycle of the waveform on E1 so that it spends greater than 50% of the cycle in the high state and the duty cycle of E2 to spend a corresponding amount of time in the low state, a net DC potential is created between the rods. Increasing or decreasing the duty cycle in this manner correspondingly changes the net DC poten-

tial between the rods [13,14]. This methodology has been used in a 3D digital ion trap to perform ion isolation [15]. However, the duty cycle of the waveforms can be changed without the high-low transitions on both rod sets happening at the same time. Fig. 2(c) reveals the method of altering the duty cycles of the waveforms to yield a net positive potential on the quadrupole electrodes. E1 begins with 60% of the time in the high state then 40% of the time in the low state while E2 begins with 40% of the time in the low state then 60% of the time in the high state. The net effect is that for 20% of the waveform period all four rods are in the high state. The rest of the cycle the device is behaving as a normal digital quadrupole ion guide. In this situation there is a competition between the dispersive effects of passing through the fringe fields (Fig. 1(a)) and the focusing effect of passing through the Einsel lens-like state while being pushed out of the quadrupole (Fig. 1(b)).

Fig. 2(d) reveals that the duty cycle of the waveforms can be adjusted to capture ions by creating a net negative potential between the end caps and the rods. This creates a linear ion trap. In this configuration, the fields created when all the rods are at the negative potential (−V) penetrate into the linear quadrupole and create a well sealed trap requiring a substantial amount of kinetic energy to escape. One of the beauties of this technique is that the linear ion guide can be instantaneously switched from trapping to ejection simply by changing the duty cycles of the waveforms.

If stopping the ions before injection into the TOF is a prerequisite for measuring high resolution TOF spectra in the ultra high mass range, the final issue is concentrating the ions before TOF injection. Ideally we would like to collect and trap the ions at the end of the multipole device just before the end cap so that they can be promptly ejected on demand in a collimated and concentrated stream into the TOF acceleration region. This requires a force along the multipole or *z*-axis to push the ions toward end cap electrode while an applied field between the end cap and the rods keeps the ions from spilling out. A field along the *z*-axis can be created by placing Linac II electrodes between the multipole rods along the field asymptotes [1]. Wilcox et al. [16] modeled the *z*-field created in this manner with tilted wires.

We performed ion trajectory calculations to show that it is possible to trap ions in a quadrupole by adjusting the duty cycle of the applied waveforms. A DC potential was applied to the Linac II electrodes to push the ions toward the exit end cap electrode. The ions collect or bunch near the end cap where the forces along the *z*-axis balance. The duty cycle of the applied digital waveforms was then be switched to eject the ions and focus them into a collimated beam for injection into the acceleration region of a TOF mass analyzer. We further demonstrated that this process can be performed at any value of *m*/*z*. These calculations demonstrate that high resolution oa-TOFMS in the ultra high mass range is feasible.

3. Simion modeling

The software used in ion trajectory modeling was SIMION 8.0 (Scientific Instrument Services, Inc., Ringoes, NJ). The linear quadrupole ion trap is modeled as shown in Fig. 3. The scaling used in the SIMION simulation was 3.95 grid units per mm (gu/mm). The dimensions of the linear ion trap are a quadrupole of 19.7 cm in length with a rod radius of 0.315 cm, and a radial distance, r_0 = 1.18 cm from the *z*-axis to the nearest surface of each rod. An end cap with a circular 3.75 cm diameter disk with 0.20 cm diameter circular hole was placed at each end of the quadrupole. Four additional electrodes called Linac II electrodes were placed between the quadrupole rods along the asymptotes. They have the shape of right triangles 1 mm thick. The hypotenuses of the triangular electrodes face the central axis of the quadrupole with the other sides parallel to the rods and end cap electrodes. The hypotenuses

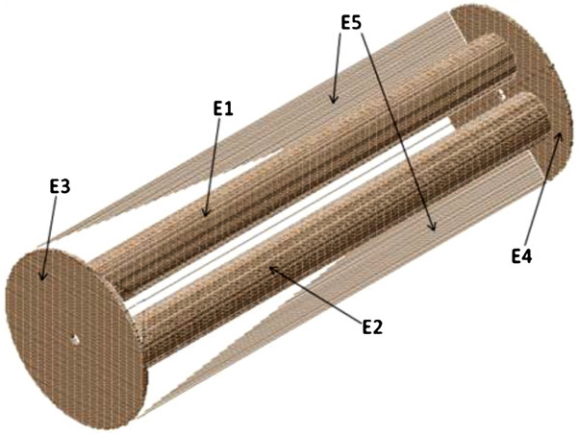

Fig. 3. A schematic of quadrupole ion trap with a set of additional electrodes used in SIMION simulations: E1 and E2, quadrupole electrodes; E3, entrance end cap; E4, exit end cap; E5, Linac II electrodes.

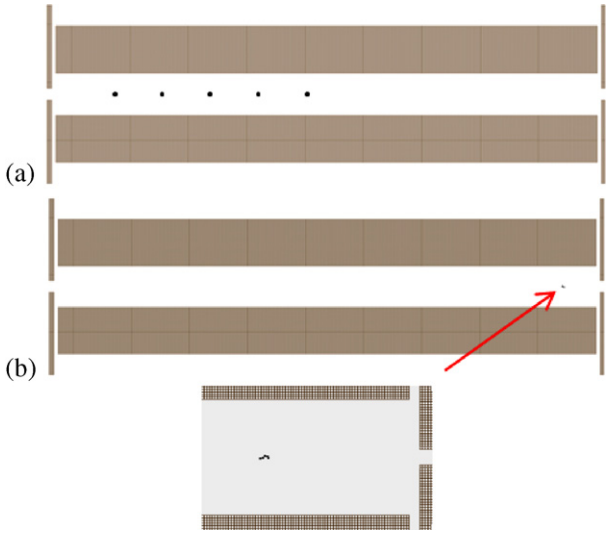

Fig. 4. Simulation of the ion bunching process used to collect the ions in front of the exit end cap for prompt ejection. (a) Ions dispersed along the central axis. The representation of the ions has been enlarged for visibility. (b) Dispersed ions collected in a spot indicated by the arrow by the interaction of the Linac II electrode potential and the trapping potential.

of the Linac II electrodes distances from the central axis range from 7.8 to 17 mm. The Five electrode sets include two opposite sets of rods (E1 and E2), entrance end cap (E3), exit end cap (E4) and the Linac II electrodes (E5). The ions examined in the simulations discussed were positive and have mass-to-charge ratios that range from 10,000 to 1,000,000. The AC voltages for ion trapping applied to E1 and E2 were 500 V and −500 V for all simulations. An axial DC voltage was added to the AC trapping potentials to adjust the kinetic energy of the ejected ions as needed. The Linac II voltages used ranged from −100 to −300 V. A nitrogen buffer gas was used at 5 and 12.5 mTorr for all simulations.

4. Simulation results

Fig. 4 illustrates the bunching process with *m*/*z* 10,000. Five ions were started inside the quadrupole on the central axis with 10 eV of kinetic energy moving toward the exit end cap electrode on the right (Fig. 4(a)). The ions were stopped by collisional cooling in a 5 mTorr N_2 buffer gas inside rods and trapped under a 60/40 of duty cycle. Therefore the 500 V trapping field is present for 20% of the

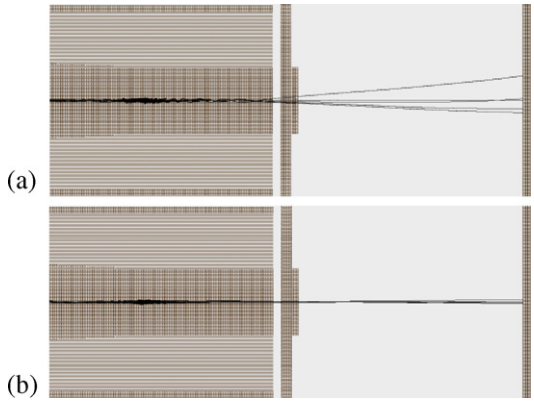

Fig. 5. Direct comparison of axial ejection with (a) 50/50 duty cycle and (b) 40/60 duty cycle. In both simulations, the ions are collected with the bunching process. The waveforms are then switched for ejection. The 50/50 duty cycle ejected the ions with 1.78 eV of kinetic energy and 24° dispersion while the 40/60 duty was used to create 1.72 eV of kinetic energy and 2° dispersion. The lighter shade reveals the profile of the Linac II electrodes.

cycle. When a −200 V of Linac II voltage was added to this trapping condition, trapped ions were focused right before the exit electrode shown in Fig. 4(b).

Once the ions were focused, two different methods were used to compare trajectories of ejected ions at the exit electrode. Fig. 5 shows distributions of model ions ejected from the quadrupole ion trap. In Fig. 5(a) the ions were first trapped and bunched in the manner described above. The quadrupole waveforms were then instantaneously switched to a 50/50 duty cycle and the Linac II voltage was set to zero. The ions ejected from the quadrupole with a 2 V DC difference between the rods and the exit end cap electrode. The ions were ejected out of the quadrupole with 1.78 ± 0.8 eV of kinetic energy with an angular spread of 24° and a temporal spread of 1174.6 ± 497.9 μs. In Fig. 5(b), the same procedure was used to trap and bunch the ions except the DC axis voltage of the quadrupole was adjusted to reduce the kinetic energy of the ejected ions for direct comparison with the 50/50 duty cycle ejection. The ions were ejected by instantaneously reversing the duty cycle to 40/60 while the −200 V Linac II voltage was maintained. As shown in Fig. 5(b), the ions were ejected out of the quadrupole with 1.72 ± 0.4 eV of kinetic energy with an angular spread of 2° and a temporal spread of 30.3 ± 2.5 μs. The difference in dispersion between the two ejection processes reveals our technique's superior ability to collimate the ejected ions. The huge difference in the temporal profiles of the ejection process reveals the advantage of our technique in terms sensitivity from coupling to a TOF analyzer.

The injection and ejection processes are theoretically independent of mass in a digitally operated quadrupole because the frequency is completely adjustable. Therefore, our trapping and injection methodology should work as well at any mass. To demonstrate this point, we examined ion injection and ejection at different masses into typical time-of-flight analyzer configuration in Fig. 6. It presents trapping and ejection of singly charged 634,875 Da ions as a function of ejection duty cycle. This mass was chosen because it represents one of the fragment ions of the proteasome complex in the work of Chernushevich and Thomson [8]. The quadrupole was operated at 100 kHz in a 12.5 mTorr background of N_2. The Linac II electrodes were set to −250 V. Fig. 6(a) shows the trapping trajectory profile of five singly charged 634,875 Da ions with 10 eV of initial kinetic energy. Fig. 6(b)–(f) shows the ejection trajectory profiles after instantaneously switching the duty cycle from trapping at 60/40 to ejection at 40/60, 30/70, 20/80 and 0/100, respectively. Notice that the collimation of the ejected ions increases as the ejection field percentage of the wave form increases from 20% at

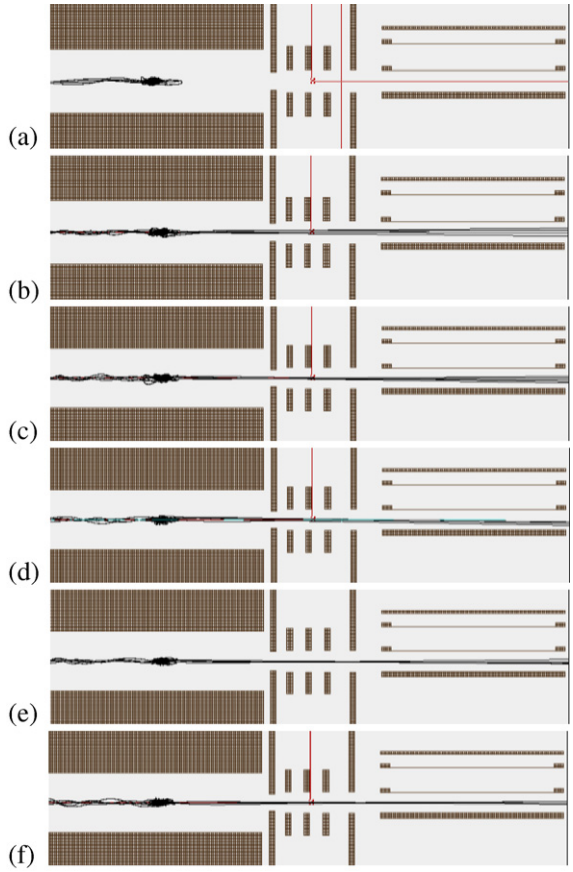

Fig. 6. Trajectory profiles of singly charged 634,875 Da ions (a) of the injection process with 10 eV initial kinetic energy and a 60/40 duty cycle. The rest show the ejection trajectories as a function of duty cycle. (b) 40/60 (c) 30/70 (d) 20/80 (e) 10/90 and (f) 0/100.

40/60 to 100% at 0/100. The collimation also increases because the dispersion-inducing fringe field components are also decreasing. We point out that although Einsel lens were included as part of the simulation, they were not energized and did not contribute to the collimation of the ion trajectories. However, they could be used in the laboratory to tune the resolution to its optimum.

In Fig. 7 the kinetic energy of the ions as a function of ejection field percentage have been plotted. The ion ejection kinetic energy increases with ejection field percentage. If there is no buffer gas

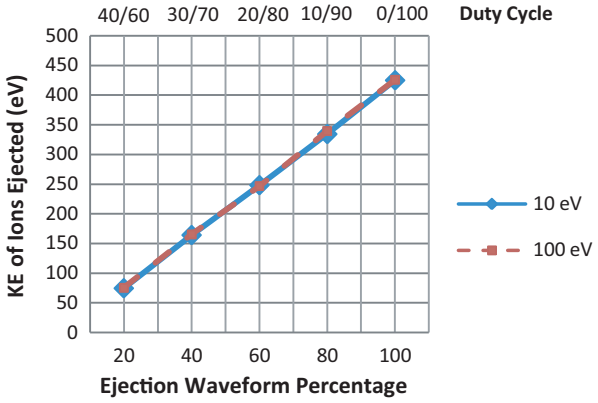

Fig. 7. The ejection kinetic energy of m/z = 634,875 ions as a function of ejection waveform percentage/duty cycle. The blue line plots the ejection energy after a 10 eV injection into 12.5 mTorr N_2 followed by bunching. The red line plots the ejection energy after a 100 eV injection into 12.5 mTorr N_2 followed by bunching.

in the device, the maximum imparted ion ejection kinetic energy would be the fraction of the ejection field times the potential difference between the DC potential of all the rods and the end cap electrode. Deviation from the maximum imparted kinetic energy values results from collisional cooling by the bath gas and the field imposed by the Linac II electrodes. The greater the gas pressure, the Linac II electrodes voltage, the cross section of the molecular ion, and/or imparted kinetic energy, the greater the deviation from the maximum imparted kinetic energy. The calculations were performed at 10 and 100 eV of initial kinetic energy injected into the quadrupole. The results of these two simulations overlay within the experimental error. It can be concluded that the ions are stopped by collisional cooling because the injection energy does not affect the ejection kinetic energy. As previously demonstrated in Fig. 5(b), the ejection kinetic energy of the ion can be compensated by the DC axis potential of the device so the ion energy can be controlled while maintaining collimation.

Our ion handling technique should also significantly increase the sensitivity of the mass spectrometers when it is applied. Transmission of ions though multipole guides and from device to device is not 100% efficient. The ability to control the kinetic energy distribution and dispersion coming out one device should markedly affect the capture probability of those ions by another guide or trap. Consequently, our technique should enhance the sensitivity of the instruments where it is applied.

5. Conclusions

Our simulation results indicate that our methodology of manipulating the duty cycle of the applied waveforms for trapping and ejection permits complete control of the kinetic energy and dispersion of the ejected ions. This method permits ions of *ANY* mass or mass-to-charge ratio to be ejected from a digitally operated quadrupole or other multipole devices in a well-collimated ion beam. Because the resolution of orthogonal acceleration time-of-flight mass analyzers primarily depends on the dispersion of the ions injected into the acceleration region and not m/z, our methodology will enable high resolution mass measurements in the ultra high mass range ($m/z > 20{,}000$). With our ion injection technique, the high resolution mass range of TOFMS should now be limited by the detector. Commercial TOF detectors are available that operate up into the megadalton range. Coupling our kinetic energy reducing inlet [17] and trapping system [9] to an oa-TOFMS and using our ion injection techniques should make high resolution mass analysis of intact singly charged proteins and protein complexes become routine.

Acknowledgement

This research was sponsored by the National Institutes of Health, NIGMS, under Grant R01 GM088501.

References

[1] A. Loboda, A. Krutchinsky, O. Loboda, J. McNabb, V. Spicer, W. Ens, K. Standing, Novel Linac II electrode geometry for creating an axial field in a multipole ion guide, European Journal of Mass Spectrometry 6 (2000) 531–536.
[2] J.B. Fenn, M. Mann, C.K. Meng, S.F. Wong, C.M. Whitehouse, Electrospray ionization for mass-spectrometry of large biomolecules, Science 246 (1989) 64–71.
[3] M. Karas, F. Hillenkamp, Laser desorption ionization of proteins with molecular masses exceeding 10000 Daltons, Analytical Chemistry 60 (1988) 2299–2301.
[4] M.P. Balogh, Debating resolution and mass accuracy, LC GC Europe 17 (2004) 152–159.
[5] R.J. Wenzel, U. Matter, L. Schultheis, R. Zenobi, Analysis of megadalton ions using cryodetection MALDI time-of-flight mass spectrometry, Analytical Chemistry 77 (2005) 4329–4337.
[6] N.J. Harmer, C.J. Robinson, L.E. Adam, L.L. Ilag, C.V. Robinson, J.T. Gallagher, T.L. Blundell, Multimers of the fibroblast growth factor (FGF)-FGF receptor-saccharide complex are formed on long oligomers of heparin, Biochemical Journal 393 (2006) 741–748.
[7] F. Sobott, H. Hernandez, M.G. McCammon, M.A. Tito, C.V. Robinson, A tandem mass spectrometer for improved transmission and analysis of large macromolecular assemblies, Analytical Chemistry 74 (2002) 1402–1407.
[8] I.V. Chernushevich, B.A. Thomson, Collisional cooling of large ions in electrospray mass spectrometry, Analytical Chemistry 76 (2004) 1754–1760.
[9] H. Koizumi, W.B. Whitten, P.T.A. Reilly, Trapping of intact, singly-charged, bovine serum albumin ions injected from the atmosphere with a 10-cm diameter, frequency-adjusted, linear quadrupole ion trap, Journal of the American Society for Mass Spectrometry 19 (2008) 1942–1947.
[10] J.H.J. Dawson, M. Guilhaus, Orthogonal-acceleration time-of-flight mass spectrometer, Rapid Communications in Mass Spectrometry 3 (1989) 155–159.
[11] R.J. Cotter, Time-of-flight mass spectrometry, in: M.J. Comstock (Ed.), ACS Symposium Series, American Chemical Society, Washington, DC, 1992.
[12] M. Guilhaus, Principles and instrumentation in time-of-flight mass spectrometry-physical and instrumental concepts, Journal of Mass Spectrometry 30 (1995) 1519–1532.
[13] J.A. Richards, R.M. Huey, J. Hiller, A new operating mode for the quadrupole mass filter, International Journal of Mass Spectrometry and Ion Physics 12 (1973) 317–339.
[14] D.J. Douglas, Linear quadrupoles in mass spectrometry, Mass Spectrometry Reviews 28 (2009) 937–960.
[15] F.L. Brancia, B. McCullough, A. Entwistle, J.G. Grossmann, L. Ding, Digital asymmetric waveform isolation (DAWI) in a digital linear ion trap, Journal of the American Society for Mass Spectrometry 21 (2010) 1530–1533.
[16] B.E. Wilcox, C.L. Hendrickson, A.G. Marshall, Improved ion extraction from a linear octopole ion trap: SIMION analysis and experimental demonstration, Journal of the American Society for Mass Spectrometry 13 (2002) 1304–1312.
[17] H. Koizumi, W.B. Whitten, P.T.A. Reilly, Controlling the expansion into vacuum—the enabling technology for trapping atmosphere-sampled particulate ions, Journal of the American Society for Mass Spectrometry 21 (2010) 242–248.